Gold Nanoparticle Effects on the Hounsfield Unit of Computed Tomography in Hepatocellular Carcinoma: Systematic Review

Pouya Gourani
Shahid Beheshti University
Amirhossein Barati Sedeh
Shahid Beheshti University
Hajar Zareyi
K.N. Toosi University of Technology
Milad Shirvaliloo
Tabriz University of Medical Sciences
Roghayeh Sheervalilou (sheervalilour@tbzmed.ac.ir)
Zahedan University of Medical Sciences
Habib Ghaznavi
Zahedan University of Medical Sciences

Research Article

Keywords: Gold Nanoparticles (AuNPs), Hepatocellular Carcinoma (HCC), Computed Tomography (CT), Image Quality, Hounsfield Unit (HU)

Posted Date: January 10th, 2022

DOI: https://doi.org/10.21203/rs.3.rs-1206225/v1

Abstract

Background: The present study has attempted to gather all the original and relevant data on the application of gold nanoparticles aimed at the improvement of computed tomography image quality and Hounsfield unit in hepatocellular carcinoma. We performed a systematic review on the studies indexed in PubMed from January 2000 to January 2020. Afterwards, the study design and quality were evaluated.

Results: An increase in the nanoparticles concentration and incubation time was associated with improved image quality and the Hounsfield Unit of computed tomography.

Conclusion: This study highlights the considerable diagnostic role of gold nanoparticle as novel contrast agents in the early detection of hepatocellular carcinoma.

Impact Statement

Early detection of cancer is still a formidable challenge. Most of the patients are diagnosed with the disease at advanced stages with metastasis, where the current therapies are rendered ineffective. Increasing the accumulation of imaging probes at the tumor site and decreasing the unwanted uptake by normal organs or the immune system are key factors for manipulating the CT image quality in a desirable way. AuNPs with considerable X-ray absorption, long circulation time and biocompatibility could be applicable for accurate and early diagnosis of malignant liver tumors and real-time monitoring of therapeutic response in near future.

Introduction

Liver cancer (Hepatocellular Carcinoma (HCC) is the fifth most common type of malignancy, and the third leading cause of cancer-related death. The annual incidence and mortality of liver cancer from 1992 to 2016, as reported by the American Cancer Society (ACS), was about 8.8 and 6.5 per 100,000 individuals per year, respectively. In 2020, 42,810 new cases of liver cancer were identified in the US, and 30,160 were reported to have died from this malignancy, indicating an incidence and mortality of 2.4% and 5.2% among cancers, respectively (https://cancer.gov). It has been estimated that liver cancer will surpass breast, prostate, and colorectal malignancies, in terms of prevalence, and become the third leading cause of cancer-related death by 2030 [1]. The overall 5-year survival rate for patients with liver cancer is only 19.6% after the disease is diagnosed. Regrettably, the majority of cases are detected in late stages, resulting in significant difficulties in the treatment process [2-5]. Interestingly, the establishment of new biomarkers can be considered for the prediction of cancer patient treatment and prognosis [6-8].

The traditional imaging methods used for detection of liver cancer include nuclear medicine imaging [9], ultrasonography [9], magnetic resonance imaging (MRI) [4, 5, 9, 10], near-infrared (NIR), Raman, single-photon emission computed tomography (SPECT) [9], positron emission tomography (PET) [9] and computed tomography (CT) [4, 5, 9-11]. Accessibility, rapidity, capability and affordability are the factors that have rendered CT an extremely valuable approach among all of these modalities [12-17]. CT can provide high-resolution images in three dimensions with great density and clarity, providing useful tomographic data. However, this method is incapable of detecting the exact boundaries of liver tumors with an acceptable accuracy [18-22].

In this regard, administration of contrast-promoting agents could be considered a helpful strategy for making a valid diagnosis with high contrast [11, 23-25]. The routine clinical CT contrast agents, as well as small iodinated compounds, are imbued with a number of challenges including short imaging time due to rapid renal clearance, renal toxicity, and inappropriate vascular permeability that have limited their applications in specific tumor imaging [26-28]. Polymer-coated bismuth sulfide (Bi_2S_3) has been demonstrated to be a good candidate for incorporation as CT contrast agent with a notable efficacy and safety higher than that of iodinated compounds [29]. However, modification of size, shape and surface area of this compound is difficult [28].

Since the prerequisite of dense matter has been regarded as a drawback for CT, it has recently been proposed to adopt materials with a high atomic number. Through the last few years, nanotechnology has widely been considered in development of theranostics [30-43]. In this respect, nanomaterials, as an increasingly trending component of nanotechnology, have left a positive impact on diagnostics, prognostics and therapeutics [44-59]. Scientists have sought to use nanoparticles (NPs) as imaging contrast agents owing to their unique physical and chemical characteristics, great biocompatibility, considerable stability and small dimensions [60-63]. According to findings, gold nanoparticles (AuNPs) possess characteristics such as plasmonic nature, non-toxicity, surface-level change, high X-ray absorption due to high atomic number [64-75], and prolonged blood circulation time [3]. These properties has distinguished them as interesting candidates for application as contrast agents [76, 77].

The present study evaluates the functional outcomes reported in the publications of the last two decades regarding the application of AuNPs as contrast agents in CT of animal models. Considering the reports included in this systematic review, we sought to provide a comprehensive discussion on the effect of properties of AuNPs such as size, shape, dosage, coating elements, effects of different injection modes, time and Hounsfield unit (HU) on liver tumor imaging. To our knowledge, no systematic review has been conducted over the past twenty years, thus, this study would be the first systematic review of the various effects of AuNPs on the quality of CT imaging of liver tumors (Figure 1).

Materials And Methods

The present study follows the PRISMA statement for transparent and comprehensive reporting of methodology and results [78].

Search strategy

All original investigations exploring the effects of AuNPs on the imaging quality of CT of liver tumors published between January 2000 and January 2020 were considered. Our keywords included “gold” AND “liver cancer” OR “hepatocarcinoma” AND “nanoparticles” OR “Nano” OR “Nano structure” OR “Nano rod” OR “Nano cage” OR “Nano shell” OR “Nano prism” OR “Nano star” OR “Nano sphere” AND “tomography” OR “computed tomography” OR “CT”.

Inclusion and exclusion criteria

All English reports concerned with the application of AuNPs as contrast agents in CT of liver tumors in both *in vitro* and *in vivo* conditions from January 2000 to January 2020 were included. In the next step, except original studies, other types of reports such as reviews, commentaries, simulation, book chapters and perspectives, studies in congresses, conferences, symposiums and incomplete articles, and papers written in languages other than English were excluded. This process was controlled and revised independently by four authors.

Data extraction

From each study, the following information were extracted: first author, year of publication, in vivo/in vitro model, administration route, AuNPs geometry/size/zeta potential/coating-conjugating agent/dose of usage/hydrodynamic size/targeting ligand/time and HU.

Quality of study

To assess the quality of observational studies included in this systematic review, a checklist as presented in Table 1, was adopted, containing 12 items with scores “Yes=1” and “No=0”. On a scale of 0 to 12 in terms of cumulative quality score, only studies with a minimum score of 8 were included in this systematic review.

Statistical analysis

Accordingly, we opted to discuss the relationship between NPs dose (mg/ml) and HU rate (r), and the correlation between NP administration time followed by CT imaging and HU rate (r).

Results

Search strategy results

As explained in Figure 2, articles were eventually included in this study [79]. According to exclusion and inclusion criteria, 13 papers were remained for analysis (Table 2 and Table 3). According to the PRISMA diagram, 741 records were found. After removing 5 duplicates, 736 records remained for further assessment. After removing 15 records including reviews, guidelines and editorials, 721 original records remained, of which 49 were irrelevant, and 657 were duplicates. The final 17 reports, after the application of the exclusion criteria, were reduced to 13 reports with potential for further evaluation.

Shape, size, cell line, coating/conjugating agents, and administration route of NPs

Most of the studies used spherical shaped NPs [2-5, 9, 11, 28, 80, 81], however, rod [82-84], and core-shell [27] and hybrid shapes [85] were also included. The preferred particle sizes were 2nm [2, 9, 11, 80] and 3nm [2, 3], but there were also reports of NPs with a size of 15nm [85], 20nm [81], 30nm [28], 80 nm [84], and 340-440 nm [83]. One of the articles reported NPs 33*9nm in size [82], and another was concerned with tiny 1nm NPs [10]. Most of the studies used HepG2 cells [2, 3, 10, 11, 81, 84], but others adopted HCC-LM3 [5, 9], SMMC-7721 [80, 83], HL-7702 [80], N1S1 [28], McA-RH7777 [82], CRL-1601 [82], BGC-823 [10], MCA-TL [85] and CHO [2] cell lines.

Regarding the NPs coating/conjugation agents, five studies incorporated polyethylene glycol (PEG) [2, 28, 81-83], two used polyethylenimine (PEI) [9, 11], two adopted silica [2, 80], two investigated dendrimer (DEN) [3, 5], another two tested lactobionic Acid (LA) [3, 84], and others reported Arginine-glycine-aspartic (RGD) [9], acetylation (Ac) [11], hyaluronic acid (HA) [5], folic acid (FA) [80], Fe_3O_4 (iron oxide) [10], amphiphilic poly; dodecyl-methacrylate-r-mPolyethyleneglycol-methylethermethacrylate-r-Methacrylic acid (DMA-r-mPEGMA-r–MA) [85], Re-Ga [81], epithelial cell adhesion molecule (EpCam) [2], polyacrilic acid (PAA) [84] and Re-Ga [81].

As for the administration route, there were eight reports on intra-venous (i.v.) [2, 3, 5, 9, 11, 28, 80, 81, 84, 85], two on intra-tumoral (i.t.) [3, 83], one on intra-peritoneal (i.p.) [3], one on intra-arterial (i.a.) [82] and one on systemic administration of NPs [10].

NP concentration, incubation time and HU rate

In articles reviewed the dose/concentration of AuNPs varied from below 1mg/ml [83] and 1mg/ml [3, 5, 80, 85] to 82 mg/ml [28]. The post-injection time followed by CT imaging varied from 0.08h [3, 10] to 48h [10], resulting in alterations in the HU from 7 [2] to 758.8 [84] without targeting, and 24 [10] to 96 [3] with targeting.

Our systematic review concluded that by increasing the NPs incubation time without targeting in animal subjects, HU rate was elevated.

Quality assessment

The scores attributed to the quality of the 13 articles included in this study fall within the acceptable range of 9 to 12 (Table 1).

Discussion

AuNPs have been reported to be great light-responsive and easily synthesized nanomaterials, with modifiable surface properties, and a thermophysical nature with tunable surface plasmon resonance (SPR). The small size renders them suitable for being accumulated within the tumor microenvironment by means of passive strategies in the treatment of cancer. AuNPs are compatible with an appreciable array of materials, have a higher X-ray absorption coefficient, and response well to different conjugates, which is particularly useful in active targeting [3, 28, 32, 80]. The present review suggests that AuNP-based contrast agents can be useful in x-ray–based computed tomography that may lead to an improvement in the HU rate.

Despite all the merits, important questions regarding the efficacy of AuNPs at improving the CT imaging quality and HU rate are yet to be answered.

The 2007 in vitro analysis by Kim *et. al.* on antibiofouling PEGylated AuNPs revealed an X-ray attenuation capacity that was 5.7 and 2 times higher than that of the routine iodine-based CT contrast agent, Ultravist, and Bi_2S_3 NPs-based agents, respectively. The fabricated NPs were used to discern hepatoma from normal liver tissue with a considerable contrast (~two-fold) 5min after injection, without imposing any alterations in the relative contrast of CT images up to 24h later [28]. In another study (2011), Kim *et. al.* demonstrated significant CT attenuation due to the hybrid constituent of amphiphilic polymer-coated Au-Fe3O4 NPs. At the same Au concentration, the HU values of the hybrid NPs were higher (723 at 100mM Au) than those of pure AuNPs (528 at 100mM Au), which was attributed to the presence of IONPs with an x-ray absorption coefficient of 0.37cm2 g^{-1} at 100keV. Moreover, the designed NPs generated a significant contrast between the hepatoma cells and normal parenchyma in CT/MRI imaging. An hour following the injection of NPs, a good contrast enhancement (~1.6fold) was achieved and the relative difference between the contrasts of the healthy and tumor tissues remained unchanged for the next 24h [85]. In 2014, Liu *et. al.* treated hepatocarcinoma cells with LA-Au DENPs, and observed a sharper enhancement in CT contrast than that elicited by non-targeted NPs at the same concentrations. An hour following the injection, a higher X-ray attenuation capacity was observed compared to that of the routine clinical iodine-based CT contrast agents at same concentrations [3]. In 2015, Zhao *et. al.* reported an HU value of 174 in CT imaging on normal mice, 30min after the injection of strawberry-like Fe3O4-Au hybrid NPs. For HCC, they observed the parenchyma with lesions highlighted through combined MRI/CT imaging after NPs administration. It was indicated that at the same concentration, Fe3O4-Au NPs displayed a higher X-ray attenuation rate than that of AuNPs [10]. A year later, Wang *et. al.* developed multifunctional HA-modified AuNPs and MnNPs for targeting CD44 receptors on HCC cells and orthotopically transplanted tumors followed by CT/MR dual-mode imaging. Their NPs exhibited good water dispersibility, great stability, cytocompatibility and high X-ray attenuation intensity. 30min following the injection of NPs, the CT intensity value of the tumors significantly increased because of the NPs being accumulated in the tumor microenvironment through the enhanced permeability and retention (EPR) effect, as well as active targeting. This enhancement partly subsided 1h into the injection of NPs [5].

In 2016, Kim *et. al.* reported from an in vitro analysis that increasing the concentration of nanocomposite microspheres improved the CT attenuation and HU in a linear manner (R2=0.9917). These nanocomplexes were infused through catheters selectively placed within the hepatic artery, and were then distributed in targeted normal liver tissues and hepatic tumors under CT imaging. The maximum intensity projection yielded a significant attenuation of HU (~205) around the tumor site [82]. Babaei *et. al.*, in 2017, reported a significant contrast enhancement in the CT images of tumors captured 6h after mouse models were injected with either EpCAM-PEG-Au@Si-5-FU, PEG-Au@Si-5-FU NPs and AuNPs (HU: 13, 7 and 0.3, respectively). In the case of PEG-Au@Si-5-FU, similar to the study mentioned earlier, this accumulation could also be attributed to the EPR effect. Nonetheless, the accumulation of EpCAM-PEG-Au@Si-5-FU at the tumor site was primarily mediated through EpCAM receptor targeting [2]. The same year, Hu *et. al.* demonstrated the superiority of the intelligent re-shieldable targeting system based on the pH-responsive self-assembly/disassembly of AuNPs. In vitro analyses showed an appreciable X-ray attenuation rate for AuNPs@Re-GA, with the CT values of the samples linearly proportionate to the concentration of AuNPs@Re-GA. The findings from preliminary CT imaging in Kunming mice with xenografted tumors disclosed that despite the CT images of tumors in both groups becoming gradually brighter, the AuNPs@Re-GA group performed better with a visual difference in the brightness compared with that of the control group. An ΔHUmax value of 41 was reported as the maximum contrast enhancement for the group treated with AuNPs@Re-GA, which was shown to be significantly higher (roughly 1.7-fold higher) than that of the control group (ΔHUmax = 23). Put together, the enhanced CT images of the tumors further indicated that the intelligent re-shieldable targeting system might be more efficient at delivering the AuNPs to the tumor site than the corresponding irreversible strategy [81]. Later that year, Wang *et. al.* mounted FA on the surface of mesoporous silica to target HCC cells and observed selective accumulation of the FA-GSJNs-DOX at the tumor site, followed by internalization. As per their findings, brighter images were obtained and an improvement was reported in CT signal intensity corresponding to FA-Au mesoporous Silica Janus (GSJNs)-doxorubicin (DOX) NPs concentration with a linear relationship (R2=0.997) [80]. In 2018, Zhou *et. al.* reported that they had observed a linear increase in CT contrast enhancement with RGD-^{99m}Tc-PEI-PEG-Au PENPs corresponding to the elevation in Au concentration in the orthotopic hepatic carcinoma models. The maximum tumor HU value was recorded 0.5h after the injection of NPs (47.1±1.8HU for targeted and 32.6±2.5HU for non-targeted), which then started to decrease slightly due to background metabolic processes. Surprisingly, the tumor HU values of the mice recorded with the RGD-Au-PENPs were remarkably greater than those recorded with the non-targeted Au PENPs at the same time points. The HU values of normal liver were also considerably greater than the orthotopic hepatic carcinoma at the same time juncture post-injection, since these particles were mainly cleared by the RES in the liver [9]. In another study, published in the same year, Zhou *et. al.* noticed that 3h post-injection, normal hepatic parenchyma (102.0±5.0HU) yielded more than 2.5 times a higher CT contrast enhancement than HCC (40.6±3.2HU). However, HCC showed a reduced tissue density as a result of the partial necrosis inside the tumor, hence, the lower CT value compared to that of the normal liver before injection [11].

Qin *et. al.* developed a novel strategy based on “seed-mediated growth” that comprised both small and large mesopores in the shell and core, respectively, with fixable Localized Surface Plasmon Resonance (LSPR) absorption and good colloidal stability in aqueous solutions, with an appreciably insignificant cytotoxic impact. Furthermore, the PEGylated multiple gold nanoparticle-encapsulated dual-mesoporous silica nanospheres PEGylated MGNRs@DMSSs, displayed a better performance as contrast agents, resulting in an image enhancement (HU=267.4) that was significantly higher than that attained with PEGylated gold nanorods (GNRs) (HU=194.8) at the same Au concentration [83]. In 2019, Zhang *et. al.* designed “Janus nanoparticles” (JNPs) with a unique surface. They investigated a distinctive nanoplatform known as LA-GNR/zeolitic imidazolate framework-8 (LA-AuNR/ZIF-8), that comprised LA-modified metallic one-dimensional nanorod/metal organic framework (1DNR/MOF) JNPs. With a one-dimentional (1D) nanostructure based on AuNRs conjugated with PAA on one

side, and modified LA on the other, LA-AuNR/ZIF-8 was shown to be an effective contrast agents, and thus, a suitable platform for targeting tumor cells, owing to its remarkable effect on the image quality of CT (HU=758.8) [84].

It is noteworthy that the enhancement of CT image quality is positively correlated with the content of contrast agent at the imaging site [81]. The retention of NPs in tumors could be enhanced by passive targeting (via the EPR effect) and active targeting, while both mechanisms work in concert to decrease the non-specific tissue biodistribution [81, 86]. However, tumor uptake of particles through active targeting has been reported to be more efficient than passive targeting. Therefore, a better quality of CT imaging can be attained with active targeting [87-89]. Traditional CT imaging agents such as barium (37.4keV) or iodine (Z=53, 33.2keV) have high X-ray absorption coefficients, nonetheless, they are known to be nephrotoxic [82]. In this regard, one may consider the conjugation, encapsulation or stabilization strategies in development of nanoplatforms facilitated with targeting ligands, imaging elements, functional moieties and antibiofouling agents [9, 28]. Generally biocompatible materials, AuNPs provide greater contrast than iodinated contrast agents, owing to their higher atomic number (Z=79) and k-edge value (80.7keV). Furthermore, the X-ray attenuation of AuNPs was not significantly reduced in water. These findings suggest a strong potential for AuNPs to serve as contrast agents in CT imaging [90]. According to an investigation by Boote et al, trivial concentrations of AuNPs, as low as a few hundred micrograms per every gram of background material (agarose), were able to result in the attenuation of X-Rays sufficient enough to change the Hu value [91].

In summary, we found that lower concentrations of AuNPs as contrast agents, compared with their traditional counterparts, result in better CT image quality and signal intensification. The elemental properties of gold in AuNPs are the major driving forces that positively affect CT contrast.

Conclusions And Future Perspective

Despite the developments in diagnostic methods, early detection of cancer is still a formidable challenge. Most of the patients are diagnosed with the disease at advanced stages with metastasis, where the current therapies are rendered ineffective. Hence, development of effective contrast agents is still a challenging task for precise early diagnosis. In this respect, increasing the accumulation of imaging probes at the tumor site and decreasing the unwanted uptake by normal organs or the immune system are key factors for manipulating the CT image quality in a desirable way. Based on novel approaches for development of nanocomplexes, the effective AuNPs with considerable X-ray absorption, long circulation time and biocompatibility have been developed for passive and active targeting aims in CT imaging of human HCC.

It can be concluded that application of gold in the form of gold nanoparticles can positively affect CT contrast compared with the more conventional contrast agents that are more heavily dependent on concentration and incubation time. Thus, application of AuNPs as contrast agents in CT could significantly enhance the image quality and provide better diagnostic results. Our systematic review showed that AuNPs could be applied for accurate and early diagnosis of malignant liver tumors and real-time monitoring of therapeutic response in near future. Different CT modalities, e.g., dual-energy CT, might as well benefit from the positive effects of AuNP-based contrast agents in the future.

Declarations

Ethics approval and consent to participate

'Not applicable'

Consent for publication

All authors are agreed.

Availability of data and materials

All data are available.

Competing interests

None

Funding

None

Authors' contributions

"All authors participated in the design, interpretation of the studies and analysis of the data and review of the manuscript; HG designed the study. PG, ABS and HZ searched the databases. PG and RS wrote the manuscript, MS edited manuscript. RS and HG revised final version.'

Acknowledgements

Thanks to Zahedan University of Medical Sciences and Iran University of Medical Sciences.

Authors' information (optional)

Permission and/or credit for reproduced images

All images are original. Permission not required. It is a systematic review manuscript. Informed consent not required.

References

1. Rahib L, Smith BD, Aizenberg R, Rosenzweig AB, Fleshman JM, Matrisian LM. Projecting cancer incidence and deaths to 2030: the unexpected burden of thyroid, liver, and pancreas cancers in the United States. *Cancer research* 2014;**74**:2913-21
2. Babaei M, Abnous K, Taghdisi SM, Amel Farzad S, Peivandi MT, Ramezani M, Alibolandi M. Synthesis of theranostic epithelial cell adhesion molecule targeted mesoporous silica nanoparticle with gold gatekeeper for hepatocellular carcinoma. *Nanomedicine* 2017;**12**:1261-79
3. Liu H, Wang H, Xu Y, Guo R, Wen S, Huang Y, Liu W, Shen M, Zhao J, Zhang G. Lactobionic acid-modified dendrimer-entrapped gold nanoparticles for targeted computed tomography imaging of human hepatocellular carcinoma. *ACS applied materials & interfaces* 2014;**6**:6944-53
4. Wang S, Huang P, Chen X. Stimuli-responsive programmed specific targeting in nanomedicine. *Acs Nano* 2016;**10**:2991-94
5. Wang R, Luo Y, Yang S, Lin J, Gao D, Zhao Y, Liu J, Shi X, Wang X. Hyaluronic acid-modified manganese-chelated dendrimer-entrapped gold nanoparticles for the targeted CT/MR dual-mode imaging of hepatocellular carcinoma. *Scientific reports* 2016;**6**:33844
6. Abdolhoseinpour H, Mehrabi F, Shahraki K, Khoshnood RJ, Masoumi B, Yahaghi E, Goudarzi PK. Investigation of serum levels and tissue expression of two genes IGFBP-2 and IGFBP-3 act as potential biomarker for predicting the progression and survival in patients with glioblastoma multiforme. *Journal of the neurological sciences* 2016;**366**:202-06
7. Shahraki K, Ahani A, Sharma P, Faranoush M, Bahoush G, Torktaz I, Gahl W, Naseripour M, Behnam B. Genetic screening in Iranian patients with retinoblastoma. *Eye* 2017;**31**:620-27
8. Kouzegaran S, Shahraki K, Makateb A, Shahri F, Hatami N, Behnod V, Tanha AS. Prognostic investigations of expression level of two genes FasL and Ki-67 as independent prognostic markers of human retinoblastoma. *Oncology research* 2017;**25**:471
9. Zhou B, Wang R, Chen F, Zhao L, Wang P, Li X, Bányai In, Ouyang Q, Shi X, Shen M. 99mTc-Labeled RGD–Polyethylenimine Conjugates with Entrapped Gold Nanoparticles in the Cavities for Dual-Mode SPECT/CT Imaging of Hepatic Carcinoma. *ACS applied materials & interfaces* 2018;**10**:6146-54
10. Zhao HY, Liu S, He J, Pan CC, Li H, Zhou ZY, Ding Y, Huo D, Hu Y. Synthesis and application of strawberry-like Fe3O4-Au nanoparticles as CT-MR dual-modality contrast agents in accurate detection of the progressive liver disease. *Biomaterials* 2015;**51**:194-207
11. Zhou B, Xiong Z, Wang P, Peng C, Shen M, Shi X. Acetylated polyethylenimine-entrapped gold nanoparticles enable negative computed tomography imaging of orthotopic hepatic carcinoma. *Langmuir* 2018;**34**:8701-07
12. Cheng Y, Morshed R, Auffinger B, Tobias AL, Lesniak MS. Multifunctional Nanoparticles for Brain Tumor Diagnosis and Therapy. *Advanced drug delivery reviews* 2013;
13. Peng C, Zheng L, Chen Q, Shen M, Guo R, Wang H, Cao X, Zhang G, Shi X. PEGylated dendrimer-entrapped gold nanoparticles for in vivo blood pool and tumor imaging by computed tomography. *Biomaterials* 2012;**33**:1107-19
14. Wang H, Zheng L, Peng C, Shen M, Shi X, Zhang G. Folic acid-modified dendrimer-entrapped gold nanoparticles as nanoprobes for targeted CT imaging of human lung adencarcinoma. *Biomaterials* 2013;**34**:470-80
15. Toth DF, Töpker M, Mayerhöfer ME, Rubin GD, Furtner J, Asenbaum U, Karanikas G, Weber M, Czerny C, Herold CJ. Rapid detection of bone metastasis at thoracoabdominal CT: accuracy and efficiency of a new visualization algorithm. *Radiology* 2013;**270**:825-33
16. Wallihan DB, Podberesky DJ, Sullivan J, Denson LA, Zhang B, Salisbury SR, Towbin AJ. Diagnostic performance and dose comparison of filtered back projection and adaptive iterative dose reduction three-dimensional CT enterography in children and young adults. *Radiology* 2015;**276**:233-42
17. Beik J, Asadi M, Mirrahimi M, Abed Z, Farashahi A, Hashemian R, Ghaznavi H, Shakeri-Zadeh A. An image-based computational modeling approach for prediction of temperature distribution during photothermal therapy. *Applied Physics B* 2019;**125**:1-13
18. Kang E-J, Kim SM, Choe YH, Lee GY, Lee K-N, Kim D-K. Takayasu arteritis: assessment of coronary arterial abnormalities with 128-section dual-source CT angiography of the coronary arteries and aorta. *Radiology* 2014;**270**:74-81
19. Tacher V, Radaelli A, Lin M, Geschwind J-F. How I do it: cone-beam CT during transarterial chemoembolization for liver cancer. *Radiology* 2015;**274**:320-34
20. Vargas HA, Miccò M, Hong SI, Goldman DA, Dao F, Weigelt B, Soslow RA, Hricak H, Levine DA, Sala E. Association between morphologic CT imaging traits and prognostically relevant gene signatures in women with high-grade serous ovarian cancer: a hypothesis-generating study. *Radiology* 2014;**274**:742-51
21. Wichmann JL, Booz C, Wesarg S, Kafchitsas K, Bauer RW, Kerl JM, Lehnert T, Vogl TJ, Khan MF. Dual-Energy CT–based phantomless in vivo three-dimensional bone mineral density assessment of the lumbar spine. *Radiology* 2014;**271**:778-84
22. Wang R, Yan Y, Zhan S, Song L, Sheng W, Song X, Wang X. Diagnosis of ovarian vein syndrome (OVS) by computed tomography (CT) imaging: a retrospective study of 11 cases. *Medicine* 2014;**93**
23. Keshavarz M, Moloudi K, Paydar R, Abed Z, Beik J, Ghaznavi H, Shakeri-Zadeh A. Alginate hydrogel co-loaded with cisplatin and gold nanoparticles for computed tomography image-guided chemotherapy. *Journal of biomaterials applications* 2018;**33**:161-69
24. Khademi S, Sarkar S, Kharrazi S, Amini SM, Shakeri-Zadeh A, Ay MR, Ghadiri H. Evaluation of size, morphology, concentration, and surface effect of gold nanoparticles on X-ray attenuation in computed tomography. *Physica Medica* 2018;**45**:127-33
25. Khademi S, Sarkar S, Shakeri-Zadeh A, Attaran N, Kharrazi S, Ay MR, Ghadiri H. Folic acid-cysteamine modified gold nanoparticle as a nanoprobe for targeted computed tomography imaging of cancer cells. *Materials Science Engineering: C* 2018;**89**:182-93

26. Prencipe G, Tabakman SM, Welsher K, Liu Z, Goodwin AP, Zhang L, Henry J, Dai H. PEG branched polymer for functionalization of nanomaterials with ultralong blood circulation. *Journal of the American Chemical Society* 2009;**131**:4783-87
27. Zhou B, Zheng L, Peng C, Li D, Li J, Wen S, Shen M, Zhang G, Shi X, interfaces. Synthesis and characterization of PEGylated polyethylenimine-entrapped gold nanoparticles for blood pool and tumor CT imaging. *ACS applied materials interfaces* 2014;**6**:17190-99
28. Kim D, Park S, Lee JH, Jeong YY, Jon S. Antibiofouling polymer-coated gold nanoparticles as a contrast agent for in vivo X-ray computed tomography imaging. *Journal of the American Chemical Society* 2007;**129**:7661-65
29. Rabin O, Perez JM, Grimm J, Wojtkiewicz G, Weissleder R. An X-ray computed tomography imaging agent based on long-circulating bismuth sulphide nanoparticles. *Nature materials* 2006;**5**:118
30. Alamzadeh Z, Beik J, Mahabadi VP, Ardekani AA, Ghader A, Kamrava SK, Dezfuli AS, Ghaznavi H, Shakeri-Zadeh A. Ultrastructural and optical characteristics of cancer cells treated by a nanotechnology based chemo-photothermal therapy method. *Journal of Photochemistry Photobiology B: Biology* 2019;**192**:19-25
31. Alamzadeh Z, Beik J, Mirrahimi M, Shakeri-Zadeh A, Ebrahimi F, Komeili A, Ghalandari B, Ghaznavi H, Kamrava SK, Moustakis C. Gold nanoparticles promote a multimodal synergistic cancer therapy strategy by co-delivery of thermo-chemo-radio therapy. *European Journal of Pharmaceutical Sciences* 2020;**145**:105235
32. Mirrahimi M, Hosseini V, Kamrava SK, Attaran N, Beik J, Kooranifar S, Ghaznavi H, Shakeri-Zadeh A. Selective heat generation in cancer cells using a combination of 808 nm laser irradiation and the folate-conjugated Fe2O3@ Au nanocomplex. *Artificial cells, nanomedicine, and biotechnology* 2018;**46**:241-53
33. Mirrahimi M, Beik J, Mirrahimi M, Alamzadeh Z, Teymouri S, Mahabadi VP, Eslahi N, Tazehmahalleh FE, Ghaznavi H, Shakeri-Zadeh A. Triple combination of heat, drug and radiation using alginate hydrogel co-loaded with gold nanoparticles and cisplatin for locally synergistic cancer therapy. *International journal of biological macromolecules* 2020;**158**:617-26
34. Mirrahimi M, Hosseini V, Shakeri-Zadeh A, Alamzadeh Z, Kamrava S, Attaran N, Abed Z, Ghaznavi H, Nami SH. Modulation of cancer cells' radiation response in the presence of folate conjugated Au@ Fe 2 O 3 nanocomplex as a targeted radiosensitizer. *Clinical Translational Oncology* 2019;**21**:479-88
35. Montazerabadi A, Beik J, Irajirad R, Attaran N, Khaledi S, Ghaznavi H, Shakeri-Zadeh A. Folate-modified and curcumin-loaded dendritic magnetite nanocarriers for the targeted thermo-chemotherapy of cancer cells. *Artificial cells, nanomedicine, biotechnology* 2019;**47**:330-40
36. Movahedi MM, Mehdizadeh A, Koosha F, Eslahi N, Mahabadi VP, Ghaznavi H, Shakeri-Zadeh A. Investigating the photo-thermo-radiosensitization effects of folate-conjugated gold nanorods on KB nasopharyngeal carcinoma cells. *Photodiagnosis photodynamic therapy* 2018;**24**:324-31
37. Sargazi S, Hajinezhad MR, Rahdar A, Zafar MN, Awan A, Baino F. Assessment of SnFe2O4 Nanoparticles for Potential Application in Theranostics: Synthesis, Characterization, In Vitro, and In Vivo Toxicity. *Materials* 2021;**14**:825
38. Barani M, Mukhtar M, Rahdar A, Sargazi S, Pandey S, Kang M. Recent advances in nanotechnology-based diagnosis and treatments of human osteosarcoma. *Biosensors* 2021;**11**:55
39. Arshad R, Barani M, Rahdar A, Sargazi S, Cucchiarini M, Pandey S, Kang M. Multi-Functionalized Nanomaterials and Nanoparticles for Diagnosis and Treatment of Retinoblastoma. *Biosensors* 2021;**11**:97
40. Barani M, Rahdar A, Sargazi S, Amiri MS, Sharma PK, Bhalla N. Nanotechnology for inflammatory bowel disease management: Detection, imaging and treatment. *Sensing and Bio-Sensing Research* 2021:100417
41. Sivasankarapillai VS, Somakumar AK, Joseph J, Nikazar S, Rahdar A, Kyzas GZ. Cancer theranostic applications of MXene nanomaterials: Recent updates. *Nano-Structures Nano-Objects* 2020;**22**:100457
42. Bilal M, Qindeel M, Raza A, Mehmood S, Rahdar A. Stimuli-responsive nanoliposomes as prospective nanocarriers for targeted drug delivery. *Journal of Drug Delivery Science Technology* 2021:102916
43. Heydari M, Yousefi AR, Nikfarjam N, Rahdar A, Kyzas GZ, Bilal M. Plant-based nanoparticles prepared from protein containing tribenuron-methyl: fabrication, characterization, and application. *Chemical Biological Technologies in Agriculture* 2021;**8**:1-11
44. Wen S, Li K, Cai H, Chen Q, Shen M, Huang Y, Peng C, Hou W, Zhu M, Zhang G. Multifunctional dendrimer-entrapped gold nanoparticles for dual mode CT/MR imaging applications. *Biomaterials* 2013;**34**:1570-80
45. Chen Q, Li K, Wen S, Liu H, Peng C, Cai H, Shen M, Zhang G, Shi X. Targeted CT/MR dual mode imaging of tumors using multifunctional dendrimer-entrapped gold nanoparticles. *Biomaterials* 2013;**34**:5200-09
46. Cai H, Li K, Li J, Wen S, Chen Q, Shen M, Zheng L, Zhang G, Shi X. Dendrimer-assisted formation of Fe3O4/Au nanocomposite particles for targeted dual mode CT/MR imaging of tumors. *Small* 2015;**11**:4584-93
47. Popovtzer R, Agrawal A, Kotov NA, Popovtzer A, Balter J, Carey TE, Kopelman R. Targeted gold nanoparticles enable molecular CT imaging of cancer. *Nano letters* 2008;**8**:4593-96
48. Barreto JA, O'Malley W, Kubeil M, Graham B, Stephan H, Spiccia L. Nanomaterials: applications in cancer imaging and therapy. *Advanced materials* 2011;**23**:H18-H40
49. Yang H, Cai W, Xu L, Lv X, Qiao Y, Li P, Wu H, Yang Y, Zhang L, Duan Y. Nanobubble–Affibody: Novel ultrasound contrast agents for targeted molecular ultrasound imaging of tumor. *Biomaterials* 2015;**37**:279-88
50. Shirvalilou S, Khoei S, Khoee S, Emamgholizadeh Minaei S. Magnetic Graphene Oxide Nanocarrier as a drug delivery vehicle for MRI monitored magnetic targeting of rat brain tumors. *Iranian Journal of Medical Physics* 2018;**15**:134-34
51. Shirvalilou S, Khoei S, Khoee S, Raoufi NJ, Karimi MR, Shakeri-Zadeh A. Development of a magnetic nano-graphene oxide carrier for improved glioma-targeted drug delivery and imaging: In vitro and in vivo evaluations. *Chemico-biological interactions* 2018;**295**:97-108

52. Irajirad R, Ahmadi A, Najafabad BK, Abed Z, Sheervalilou R, Khoei S, Shiran MB, Ghaznavi H, Shakeri-Zadeh A. Combined thermo-chemotherapy of cancer using 1 MHz ultrasound waves and a cisplatin-loaded sonosensitizing nanoplatform: an in vivo study. *Cancer Chemotherapy Pharmacology* 2019:1-7
53. Saravani R, Sargazi S, Saravani R, Rabbani M, Rahdar A, Taboada P. Newly crocin-coated magnetite nanoparticles induce apoptosis and decrease VEGF expression in breast carcinoma cells. *Journal of Drug Delivery Science and Technology* 2020;**60**:101987
54. Rahdar A, Hajinezhad MR, Sargazi S, Bilal M, Barani M, Karimi P, Kyzas GZ. Biochemical effects of deferasirox and deferasirox-loaded nanomicellesin iron-intoxicated rats. *Life Sciences* 2021;**270**:119146
55. Rahdar A, Sargazi S, Barani M, Shahraki S, Sabir F, Aboudzadeh MA. Lignin-stabilized doxorubicin microemulsions: Synthesis, physical characterization, and in vitro assessments. *Polymers* 2021;**13**:641
56. Rahdar A, Hajinezhad MR, Bilal M, Askari F, Kyzas GZ. Behavioral effects of zinc oxide nanoparticles on the brain of rats. *Inorganic Chemistry Communications* 2020;**119**:108131
57. Shirvalilou S, Khoei S, Khoee S, Emamgholizadeh Minaei S. Magnetic Graphene Oxide Nanocarrier as a drug delivery vehicle for MRI monitored magnetic targeting of rat brain tumors. *Iranian Journal of Medical Physics* 2018;**15**:134-34
58. Arshad R, Tabish TA, Kiani MH, Ibrahim IM, Shahnaz G, Rahdar A, Kang M, Pandey S. A Hyaluronic Acid Functionalized Self-Nano-Emulsifying Drug Delivery System (SNEDDS) for Enhancement in Ciprofloxacin Targeted Delivery against Intracellular Infection. *Nanomaterials* 2021;**11**:1086
59. Javad Farhangi M, Es-Haghi A, Taghavizadeh Yazdi ME, Rahdar A, Baino F. MOF-Mediated Synthesis of CuO/CeO2 Composite Nanoparticles: Characterization and Estimation of the Cellular Toxicity against Breast Cancer Cell Line (MCF-7). *Journal of Functional Biomaterials* 2021;**12**:53
60. Nune SK, Gunda P, Thallapally PK, Lin Y-Y, Laird Forrest M, Berkland CJ. Nanoparticles for biomedical imaging. *Expert opinion on drug delivery* 2009;**6**:1175-94
61. Neshastehriz A, Tabei M, Maleki S, Eynali S, Shakeri-Zadeh A. Photothermal therapy using folate conjugated gold nanoparticles enhances the effects of 6 MV X-ray on mouth epidermal carcinoma cells. *Journal of Photochemistry and Photobiology B: Biology* 2017;**172**:52-60
62. Rauf A, Tabish TA, Ibrahim IM, ul Hassan MR, Tahseen S, Sandhu MA, Shahnaz G, Rahdar A, Cucchiarini M, Pandey S. Design of Mannose-Coated Rifampicin nanoparticles modulating the immune response and Rifampicin induced hepatotoxicity with improved oral drug delivery. *Arabian Journal of Chemistry* 2021;**14**:103321
63. Fiume E, Magnaterra G, Rahdar A, Verné E, Baino F. Hydroxyapatite for Biomedical Applications: A Short Overview. *Ceramics* 2021;**4**:542-63
64. Astolfo A, Schültke E, Menk RH, Kirch RD, Juurlink BH, Hall C, Harsan L-A, Stebel M, Barbetta D, Tromba G. In vivo visualization of gold-loaded cells in mice using x-ray computed tomography. *Nanomedicine: Nanotechnology, Biology and Medicine* 2013;**9**:284-92
65. Diaz RJ, McVeigh PZ, O'Reilly MA, Burrell K, Bebenek M, Smith C, Etame AB, Zadeh G, Hynynen K, Wilson BC. Focused ultrasound delivery of Raman nanoparticles across the blood-brain barrier: potential for targeting experimental brain tumors. *Nanomedicine: Nanotechnology, Biology and Medicine* 2014;**10**:e1075-e87
66. Thakor A, Jokerst J, Zavaleta C, Massoud T, Gambhir S. Gold nanoparticles: a revival in precious metal administration to patients. *Nano letters* 2011;**11**:4029-36
67. Beik J, Shiran MB, Abed Z, Shiri I, Ghadimi-Daresajini A, Farkhondeh F, Ghaznavi H, Shakeri-Zadeh A. Gold nanoparticle-induced sonosensitization enhances the antitumor activity of ultrasound in colon tumor-bearing mice. *Medical physics* 2018;**45**:4306-14
68. Hashemian A, Eshghi H, Mansoori G, Shakeri-Zadeh A, Mehdizadeh A. Folate-conjugated gold nanoparticles (synthesis, characterization and design for cancer cells nanotechnology-based targeting). *International Journal of Nanoscience Nanotechnology* 2009;**5**:25-34
69. Mirrahimi M, Khateri M, Beik J, Ghoreishi FS, Dezfuli AS, Ghaznavi H, Shakeri-Zadeh A. Enhancement of chemoradiation by co-incorporation of gold nanoparticles and cisplatin into alginate hydrogel. *Journal of Biomedical Materials Research Part B: Applied Biomaterials* 2019;**107**:2658-63
70. Neshastehriz A, Khateri M, Ghaznavi H, Shakeri-Zadeh A. Investigating the therapeutic effects of alginate nanogel co-loaded with gold nanoparticles and cisplatin on U87-MG human glioblastoma cells. *Anti-Cancer Agents in Medicinal Chemistry* 2018;**18**:882-90
71. Neshastehriz A, Khosravi Z, Ghaznavi H, Shakeri-Zadeh A. Gold-coated iron oxide nanoparticles trigger apoptosis in the process of thermo-radiotherapy of U87-MG human glioma cells. *Radiation environmental biophysics* 2018;**57**:405-18
72. Shakeri-Zadeh A, Eshghi H, Mansoori G, Hashemian A. Gold nanoparticles conjugated with folic acid using mercaptohexanol as the linker. *Journal Nanotechnology Progress International* 2009;**1**
73. Rajaee Z, Khoei S, Mahdavian A, Shirvalilou S, Mahdavi SR, Ebrahimi M. Radio-thermo-sensitivity Induced by Gold Magnetic Nanoparticles in the Monolayer Culture of Human Prostate Carcinoma Cell Line DU145. *Anti-Cancer Agents in Medicinal Chemistry* 2020;**20**:315-24
74. Changizi O, Khoei S, Mahdavian A, Shirvalilou S, Mahdavi SR, Rad JK. Enhanced radiosensitivity of LNCaP prostate cancer cell line by gold-photoactive nanoparticles modified with folic acid. *Photodiagnosis photodynamic therapy* 2020;**29**:101602
75. Hassanisaadi M, Bonjar GHS, Rahdar A, Pandey S, Hosseinipour A, Abdolshahi R. Environmentally Safe Biosynthesis of Gold Nanoparticles Using Plant Water Extracts. *Nanomaterials* 2021;**11**:2033
76. Cheng Y, Dai Q, Morshed RA, Fan X, Wegscheid ML, Wainwright DA, Han Y, Zhang L, Auffinger B, Tobias AL. Blood-brain barrier permeable gold nanoparticles: an efficient delivery platform for enhanced malignant glioma therapy and imaging. *Small* 2014;**10**:5137-50
77. Dixit S, Novak T, Miller K, Zhu Y, Kenney ME, Broome A-M. Transferrin receptor-targeted theranostic gold nanoparticles for photosensitizer delivery in brain tumors. *Nanoscale* 2015;**7**:1782-90
78. Moher D, Liberati A. A., Tetzlaff, J., & Altman, DG (2009). Preferred reporting items for systematic reviews and meta-analyses: the PRISMA statement. *BMJ* **339**:b2535

79. Liberati A, Altman DG, Tetzlaff J, Mulrow C, Gøtzsche PC, Ioannidis JP, Clarke M, Devereaux PJ, Kleijnen J, Moher D. The PRISMA statement for reporting systematic reviews and meta-analyses of studies that evaluate health care interventions: explanation and elaboration. *PLoS medicine* 2009;**6**:e1000100
80. Wang Z, Shao D, Chang Z, Lu M, Wang Y, Yue J, Yang D, Li M, Xu Q, Dong W-f. Janus gold nanoplatform for synergetic chemoradiotherapy and computed tomography imaging of hepatocellular carcinoma. *ACS nano* 2017;**11**:12732-41
81. Hu Z, Ma J, Fu F, Cui C, Li X, Wang X, Wang W, Wan Y, Yuan Z. An intelligent re-shieldable targeting system for enhanced tumor accumulation. *Journal of Controlled Release* 2017;**268**:1-9
82. Kim D-H, Li W, Chen J, Zhang Z, Green RM, Huang S, Larson AC. Multimodal imaging of nanocomposite microspheres for transcatheter intra-arterial drug delivery to liver tumors. *Scientific reports* 2016;**6**:29653
83. Qin L, Niu D, Jiang Y, He J, Jia X, Zhao W, Li P, Li Y. Confined growth of multiple gold nanorices in dual-mesoporous silica nanospheres for improved computed tomography imaging and photothermal therapy. *International journal of nanomedicine* 2019;**14**:1519
84. Zhang H, Zhang Q, Liu C, Han B. Preparation of a one-dimensional nanorod/metal organic framework Janus nanoplatform via side-specific growth for synergistic cancer therapy. *Biomaterials science* 2019;**7**:1696-704
85. Kim D, Yu MK, Lee TS, Park JJ, Jeong YY, Jon S. Amphiphilic polymer-coated hybrid nanoparticles as CT/MRI dual contrast agents. *Nanotechnology* 2011;**22**:155101
86. Mura S, Nicolas J, Couvreur P. Stimuli-responsive nanocarriers for drug delivery. *Nature materials* 2013;**12**:991
87. Nicolas J, Mura S, Brambilla D, Mackiewicz N, Couvreur P. Design, functionalization strategies and biomedical applications of targeted biodegradable/biocompatible polymer-based nanocarriers for drug delivery. *Chemical Society Reviews* 2013;**42**:1147-235
88. Peer D, Karp JM, Hong S, Farokhzad OC, Margalit R, Langer R. Nanocarriers as an emerging platform for cancer therapy. *Nature nanotechnology* 2007;**2**:751
89. Kamaly N, Xiao Z, Valencia PM, Radovic-Moreno AF, Farokhzad OC. Targeted polymeric therapeutic nanoparticles: design, development and clinical translation. *Chemical Society Reviews* 2012;**41**:2971-3010
90. Chen H, Rogalski MM, Anker JN. Advances in functional X-ray imaging techniques and contrast agents. *Physical Chemistry Chemical Physics* 2012;**14**:13469-86
91. Boote E, Fent G, Kattumuri V, Casteel S, Katti K, Chanda N, Kannan R, Katti K, Churchill R. Gold nanoparticle contrast in a phantom and juvenile swine: models for molecular imaging of human organs using x-ray computed tomography. *Academic radiology* 2010;**17**:410-17

Tables

Table 1. Items of quality assessment chosen from QUADAS checklist

Questions	Yes=1	No=0
1. Are the research questions clearly stated?		
2. Is the approach appropriate for the research question?		
3. Is the study context clearly described?		
4. Is the role of the researcher clearly described?		
5. Is the sampling method clearly described?		
6. Is the sampling strategy appropriate for the research question?		
7. Is the data collection method clearly described?		
8. Is the data collection method appropriate to answer the research question?		
9. Is the method of analysis clearly described?		
10. Are the main characteristics of the population well described?		
11. Is the analysis appropriate for the research question?		
12. Are the claims made supported by sufficient evidence?		

Table 2. Overview of CT imaging studies conducted using AuNPs by dose (all references within the tables are included in the References section, and include the reference # in the table)

Reference	Administration Route	Cell Line	Geometry	Size (nm)	Zeta Potential (mv)	Coating/ Conjugation	NP Dose (mg/ml)	*Hounsfield Unit*	Quality Assessment
#Liu *et al.* 2014 Ref: 3	i.p. i.v. i.t.	HepG2	Spherical	3	4	DEN/LA	1 2 4 8 12 16	62 93 197 364 536 702	12
#Zhou *et al.* 2018 Ref: 6	i.v.	HCC-LM3	Spherical	2	111	PE/RGD	20	47	12
#Zhou *et al.* 2018 Ref: 8	i.v.	HepG2	Spherical	2	16	PE/Ac	2 7 11 16 20	125 254 374 504 610	9
#Wang *et al.* 2016 Ref: 5	i.v.	HCCLM3	Spherical	2	6	DEN/HA	2 4 6 1 24	30 76 168 350 692	11
#Wang *et al.* 2017, Ref: 67	i.v.	SMMC-7721 , HL-7702	Spherical	2	Not Mentioned	Silica /FA	0 0 1 3 5 10	22 27 31 43 65 127	10
#Kim *et al.* Ref: 25	i.v.	N1S1 , HepG2	Spherical	30	Not Mentioned	PEG	4 82 16	143 178 418	11
#Kim *et al.* 2016 Ref: 69	i.a.	McA-RH7777 , CRL-1601	Rod	33 × 9	− 42	PEG	5 15 30 50 60	64 98 156 243 289	12
#Zhao *et al.* 2015 Ref: 7	Administrated systematically	BGC-823 , HepG2	Core-Shell	1 (shell thickness)	Not Mentioned	Fe_3O_4	3 8 19 35	169 408 963 173	12
#Kim *et al.* 2011 Ref: 72	i.v.	MCA-TL	Hybrid	15	Not Mentioned	poly(DMA-r-mPEGMA-r – MA)	0 1 2 10 20	0 37 104 403 723	12
#Qin *et al.* 2019 Ref: 70	i.t.	In vivo	Rod	aspect ratio: 3.7-4 (340-440)	Not Mentioned	PEGylated MGNRs@DMSSs	5.3	67	12
#Qin *et al.* 2019 Ref: 70	-	SMMC-7721	Rod	aspect ratio: 3.7-4 (340-440)	Not Mentioned	PEGylated MGNRs@DMSSs	0.3 0.9 1.4 2.4 4.5	21.5 47.4 79.8 141.2 267.4	
						PEGylated GNRs	0 0.5	20.5 45.4	

							1.1	58.4	
							2.2	106.1	
							4.5	194.8	
#Zhang et al.	i.v.	HepG-2 cells,	Rod	80	Not Mentioned	LA-AuNR/ZIF-8	0.1	100	12
2019		MCF-7					3.8	141.1	
Ref: 71							7.7	186.2	
							15	268.6	
							30	431.3	
							60.1	758.8	

Abbreviations;

Ac: Acetylation, AuNPs: gold nanoparticles, AuNRs: gold nanorods, CT: computed tomography, DEN: Dendrimer, DMA: Dodecyl methacrylate, FA: Folic acid, Fe3O4: iron oxide, GNRs: gold nanorods, HA: Hyaluronic acid, i.a.: Intra-Arterial, i.p.: Intraperitoneally, i.t.: Intratumorally, i.v.: Intravenously, LA: Lacto bionic Acid, MA= Methacrylic acid, MGNRs@DMSSs: multiple gold nanorices-encapsulated dual-mesoporous silica nanospheres (designated as PEGylated MGNRs@DMSSs), NP: Nanoparticle, PE: Polyethylenimine, PEG: polyethylene glycol, PEGMA: Poly (ethylene glycol) methyl ether methacrylate, RGD: Arginine-glycine-aspartic, ZIF-8: zeolitic imidazolate framework-8

Table 3. Overview of CT imaging studies conducted using AuNPs by time (all references within the tables are included in the References section, and include the reference # in the table)

Reference	Administration Route	Cell Line	NP Geometry	NP Size (nm)	Zeta Potential (mv)	NP Coating/ Conjugation	Type of Contrast	Time (h)	*Hounsfield unit* Without/with targeting		Quality assessment
#Liu *et al.* 2014 Ref: 3	i.p. i.v. i.t.	HepG2	Spherical	3	4	DEN/LA	Positive	0.08 0.5 1 1.5 2	51 59 78 54 46	67 82 92 67 62	12
#Zhou *et al.* 2018 Ref: 6	i.v.	HCC-LM3	Spherical	2	11	PE/RGD	Positive	0 0.5 2 5	27 33 32 26	24 47 44 37	12
#Zhou *et al.* 2018 Ref: 8	i.v.	HepG2	Spherical	2	16	PE/Ac	Negative	0 0.5 1 1.5 2 2.5 3	54 73 81 86 97 100 102	37 54 53 49 48 43 41	9
#Wang *et al.* 2016 Ref: 5	i.v.	HCCLM3	Spherical	2	6	DEN/HA	Positive	0 0.5 1 2	48 56 52 50	48 66 61 56	11
#Hu *et al.* 2017 Ref: 67	i.v.	HepG2	Spherical	20	not mentioned	PEG/Re-GA	Positive	0 1 2 3 5	44 64 80 84 58	41 44 52 63 48	11
#Babaei *et al.* 2017 Ref: 2	i.v.	HepG2 , CHO	Spherical	2-3	11	PEG- Silica / EpCAM	Positive	6 24	7 13	-	12
#Zhao *et al.* 2015 Ref: 7	administrated systematically	BGC-823 , HepG2	Core-Shell	1 (shell thickness)	not mentioned	Fe_3O_4	Positive	pre 0.08 0.25 0.5 1 8 24 48	10 133 167 175 164 160 157 153	-	12

Abbreviations;

Ac: Acetylation, AuNPs: gold nanoparticles, AuNPs@Re-GA: gold nanoparticles modified with liver tumor targeting ligand glycyrrhetinic Acid, CT: computed tomography, DEN: Dendrimer, EpCAM: Epithelial cell adhesion molecule, FA: Folic acid, Fe3O4: iron oxide, GA= glycyrrhetinic acid, HA: Hyaluronic acid, i.p.: Intraperitoneally, i.t.: Intratumorally, i.v.: Intravenously, LA: Lacto bionic Acid, NP: Nanoparticle, PE: Polyethylenimine, PEG: polyethylene glycol, RGD: Arginine-glycine-aspartic,

Figures

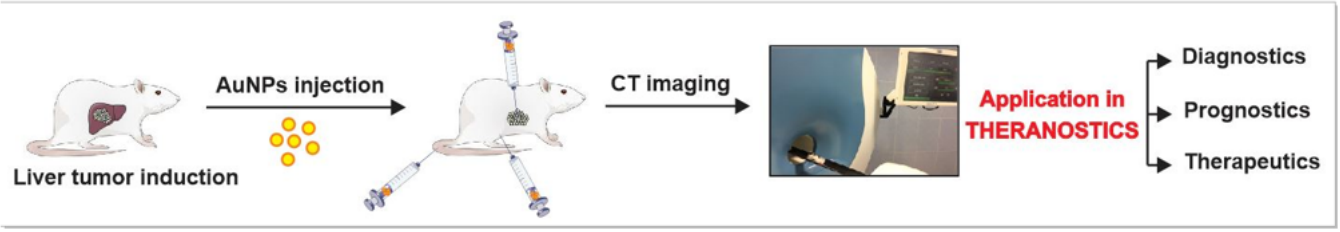

Figure 1

Application of AuNPs in theranostics.

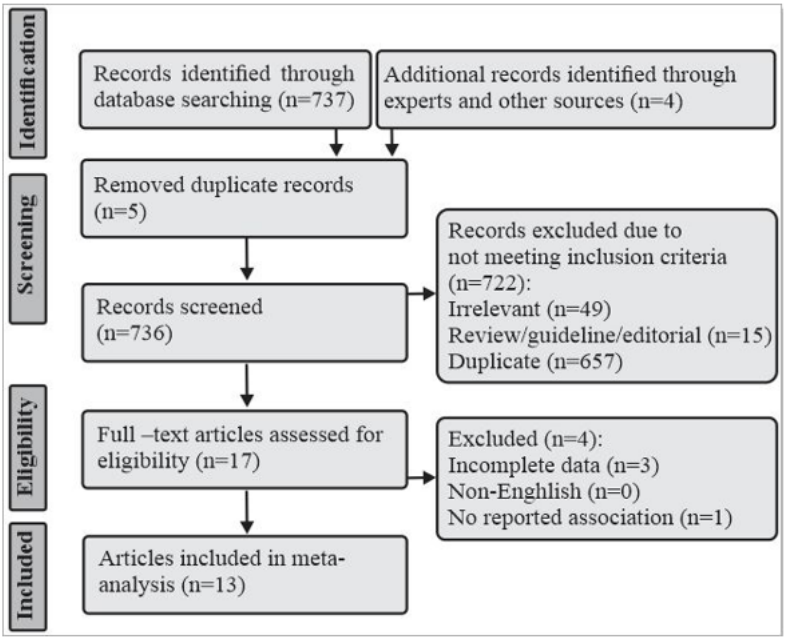

Figure 2

Tree diagram of study selection based on PRISMA criteria